30th November 2023. Vol.67 No.3 © 2012 ISOMAse, All rights reserved

November 30, 2023

The Effect of Variation of Bar Surface Chamfer Angle on Rotary Friction Welding Connections

Yohanes,^{a,*} Muftil Badri^{a,} and Syafirman Pramija^a

a) Mechanical Engineering Department, Faculty of Engineering, Universitas Riau, Indonesia

*Corresponding author: yohanes@lecturer.unri.ac.id

Paper History

Received: 07-October-2022

Received in revised form: 15-May-2023

Accepted: 30-November-2023

ABSTRACT

This study aims to determine the effect of chamfer angle variations on flash, welding time, interface and hardness values at welded joints of similar materials. The method was used, with parameters of the rotational speed of 4.335 rpm, friction pressure of 0.5 MPa, forging pressure of 0.7 MPa, forging time of 10 seconds and chamfer angle variations of 0°, 15°, 30°, 45°. Then, the specimen result was tested using the projector profile, Non-Destructive Test (NDT), macro-observation, and Vicker test. The result showed that the greater the chamfer angle variation on the given bar surface, the smaller the size of the resulting flash. The smallest flash dimension was produced at a chamfer angle variation of 45°, with an average flash height of 1.03 mm, successfully reducing the flash height by 62% from variations without chamfer angles. Moreover, an average flash width of 0.26 mm reduced the flash width by 77% of the variation without a chamfer angle. Therefore, the greater the variation of the chamfer angle, the smaller the flash size and the more significant the variation of the chamfer angle, the longer the welding time. In the interface area, chamfer angle variations do not affect cracks and voids. The chamfer angle affects the average hardness value, where the more significant the chamfer angle, the more the hardness value is increased.

KEYWORDS: Rotary friction welding, Bar-plate, Chamfer angle, Flash.

1.0 INTRODUCTION

The development of welding technology is required to produce metal joining processes in various forms, types of materials and constructions in increasingly complex industrial products. One widely used material is mild steel AISI 1037, classified as carbon steel with iron and carbon alloy elements. This type of alloy can be given heat treatment and has good cutting properties. However, the connection of mild steel has problems if it is done using the liquid welding method, where the connection process requires filler metal as the connecting medium, and penetration occurs only around it so that the connection strength is not the same as the parent metal [1]. Mild steel bar-plate connection products include iron door frames and iron fences, bridge construction, shaft connections, and others. The method that can be used to overcome this problem is the friction welding method.

Friction welding is the joining of two metals by utilizing the heat energy generated from the friction of the two materials [2-7]. One metal rotates at a certain speed, and the other is given pressure so that the two metals rub against each other, producing heat so that the splicing process occurs. The friction between the surfaces allows a rapid rise in temperature at the joint surfaces, causing the mass to undergo plastic deformation and travel based on applying pressure and centrifugal force, creating a flash [8-10]. The advantage of friction welding is that the welding temperature is low and does not use flux/welding membrane, gas and filler/electrode. The welding process is carried out in a solid state, so there are no sparks or smoke.

Moreover, the advantage of friction welding is savings in filler metal and time for joining two similar or different materials. Meanwhile, the critical process parameters are friction, pressure, forging, and rotational speed [11-14]. In this joining process, plastic deformation occurs due to forging pressure, and a diffusion process occurs due to high heat, resulting in a high-quality connection between similar and different materials.

The friction welding machine used in this paper was a vertical bar-plate rotary friction welding machine designed by Utamar and Siswanto [15]. This machine connects bar-shaped and plate-shaped materials by utilizing machine rotation and pneumatic compressive forces. They conducted the machine testing, and the bar-plate rotary friction welding machine was successfully operating with good performance based on the design and manufacture that had been determined [15]. In addition to simplifying the work process, friction welding aims to obtain optimal efficiency. All friction welding processes will always produce a flash shaped like a ring. The more flashes that appear, the more production costs will increase [16-18]. However, when testing was carried out by [15] using an upright

30th November 2023. Vol.67 No.3 © 2012 ISOMAse, All rights reserved November 30, 2023

bar-plate rotary friction welding machine, all specimens were limited by the parameter variation of the bar surface chamfer angle of 0° (without chamfer angle) and the test results produced residual welding results or flash. Further investigation for chamfer angle variation must be known to reduce the resulting flash. Therefore, this paper aims to determine the effect of chamfer angle variations on flash, welding time, interface and hardness values at welded joints of similar materials.

2.0 METHODOLOGY

In this study, the experimental method was adopted to analyze the effect of chamfer angle variations on flash, welding time, interface and hardness values at welded joints of similar materials. The material used for specimens was the mild steel AISI 1037. The tools and materials used such as bar-plate upright rotary friction welding machine, compressor, lathe machine, hand grinder, jig and fixture, projector profile, vernier calliper, protractor, stopwatch, tachometer, optical microscope, hardness tester machine, remover, penetrant and developer, lathe chisel, sandpaper, and etching solution.

2.1 Creating a Chamfer Angle

This stage made the workpiece for the experiments. It was connected according to the dimensions and sizes of the chamfer angles shown in Figure 1.

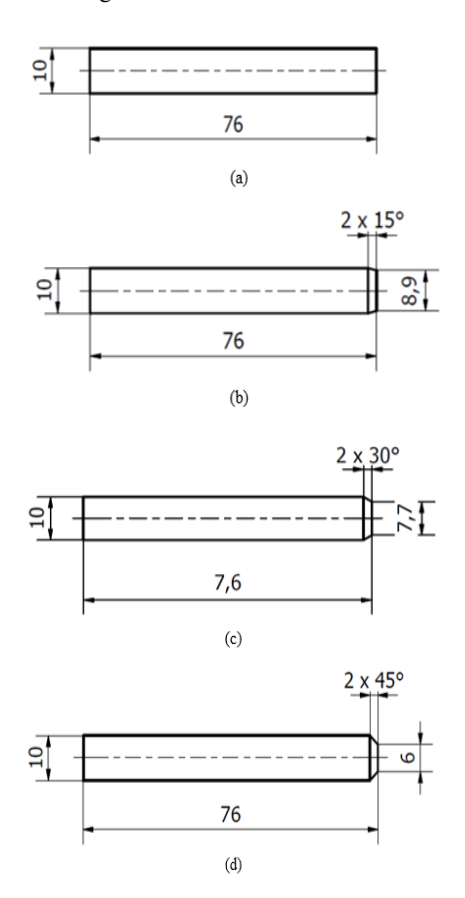


Figure 1: The specimens job sheet (a) no corner Chamfer (b) chamfer 15° (c) chamfer 30° (d) chamfer 45°

2.2 The Welding Procedure Process

The welding procedure using an upright bar-plate rotary friction welding machine is as follows: 1. Prepare tools and materials to be used in the welding process using a bar-plate vertical friction welding machine; 2. Set up the bar-plate upright rotary friction welding machine, 3. Spindle speed is regulated by changing the order of the v-belts on the pulleys, 4. The workpiece bar or rod is inserted into the spindle and then tightened 5. The pressure applied to the bar-plate upright rotary friction welding machine is regulated, 6. The spindle rotation is turned on, and the stopwatch is turned on to determine friction and forging times. 7. The pneumatic valve is pressed until the material rubs together. 8. After that, the pneumatic pressure is increased to perform the forging pressure by turning the pressure regulator on the bar-plate upright rotary friction welding machine until it reaches a pressure of 0.7 MPa while still pressing the pneumatic lever and then doing it for 10 seconds. An example of the welding process is shown in Figure



Figure 2: The welding process

2.3 Result of Welding Test 2.3.1 Flash Dimension

The process of measuring flash dimensions using a projector profile was as follows: 1.100x magnification lens mounted on projector profile. The flash's height and width were measured by rotating the cross-slide and the upper-slide to the desired point. The image was seen on the projector's profile monitor and then was observed by continuously rotating the X and Y swivel until the desired point. Finally, the numbers listed on the X and Y sash were collected. This procedure was repeated until all the desired points were known. The flash dimension measurement process is depicted in Figure 3.

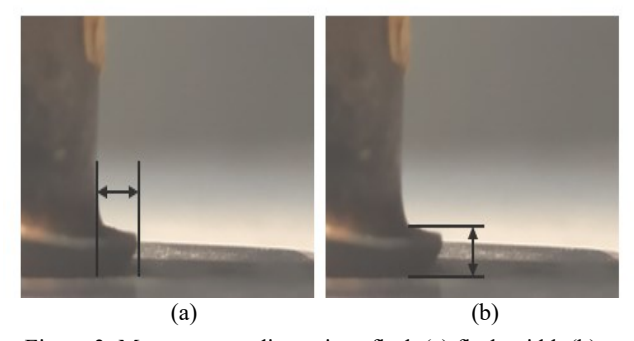


Figure 3: Measurement dimensions flash (a) flash width (b) flash height

30th November 2023. Vol.67 No.3 © 2012 ISOMAse, All rights reserved November 30, 2023

2.3.2 Non-Destructive Test (NDT)

The procedure for testing using the liquid penetrant testing method (Figure 4): 1. Cleaning the specimen using a liquid remover, 2. Penetrant administration was carried out after the liquid remover was completely dry, and then the liquid penetrant was on the specimen until it was evenly distributed.

3. After giving the penetrant, the next step was to clean the penetrant using a liquid remover; 4. After the specimen was clean, the next step was to give the developer fluid, 5. Repeat steps 1 to 4 until all welded specimens have been tested.



Figure 4: Developer rewards

2.3.3 Metallography

The stages of the process of observing the microstructure were as follows:

1. Sample cutting stage. At this stage, the test specimen is first cut until it reaches the core of the weld (Figure 5).



Figure 5: The cutting result of the specimens

- 2. Sanding and polishing stages. At this stage, the test specimens that have been cut will first be sanded. The sanding process starts from the coarsest sandpaper grade of 80 mesh, 100 mesh, 150 mesh, 240 mesh, 400 mesh, 600 mesh, 800 mesh, 1000 mesh, 1500 mesh, and 2000 mesh in stages,
- 3. Stage of making etching solution. Etching in the form of a solution that serves to bring up the phase and or grain boundaries. Each type of metal material uses a different etching fluid. Generally, the etching fluid used is Nital 2% for iron and steel
- 4. Etching or etching stage. This stage is the stage of giving the etching solution to the test specimen. The time given during the etching process using 2% Nital is 60 seconds for welding material.
- 5. Macro observation stage. At this stage, the test specimen that has been given an etching solution,
- 6. Observed using an optical microscope with a magnification of 5x.

2.3.4 Hardness Test

This hardness test was carried out to determine the hardness value of a test material that has been welded. This hardness test

used the Vickers method, which the Vickers hardness test method used an indenter in the form of an inverted diamond pyramid, which has a peak angle of 136°. The indenter was pressed against the test material under a load of 60 kgf for 60 seconds. Then, resulting in a trace that an optical microscope lens can measure its. The hardness test is shown in Figure 6.

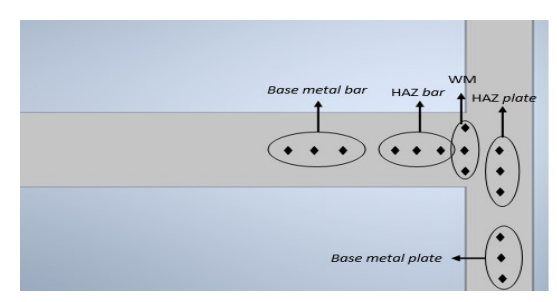


Figure 6: Hardness test

Finally, the data results of many tests were compared, and the effect of variations in the bar surface chamfer angle was analyzed.

3.0 RESULTS AND DISCUSSION

3.1 Welding Time and Flash Dimension Result

Figure 7 shows the friction time of the rotary friction welding bar plate. Figure 7 shows the increase in friction time from no chamfer angle to 45° chamfer angle and gets the average friction time.

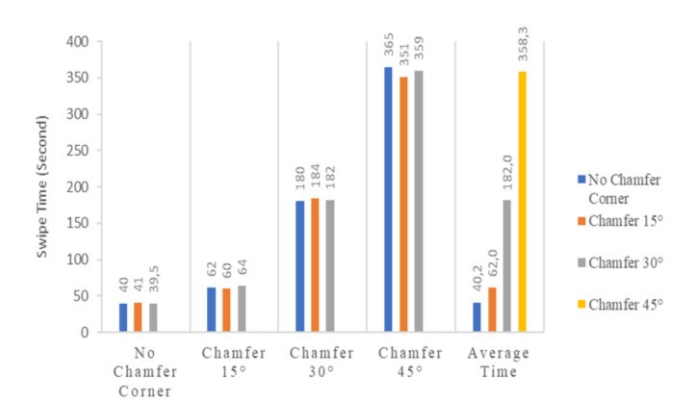


Figure 7: Friction time rotary friction welding bar-plate

Figure 7 depicts the average friction time obtained from the three welding specimens for each variation of the chamfer angle, which is the variation without the chamfer angle (0° or 180°). The time obtained was 40.16 seconds. Then, at the chamfer angle variation of 15°, the time was obtained by 62 seconds, the variation of the chamfer angle of 30° obtained a time of 182 seconds, and the variation of the chamfer angle of 45° obtained a time of 358.33 seconds. Friction time was seen from the phenomena that occur during the welding process. Therefore, it can be concluded that the greater the chamfer angle, the longer the friction time. The increase in friction time is caused by the relationship between the chamfer angle and the

30th November 2023. Vol.67 No.3 © 2012 ISOMAse, All rights reserved November 30, 2023

heat input value during the welding process, which is inversely proportional to where the more significant the chamfer angle, the smaller the heat input value generated during the welding process. The relationship between the chamfer angle and the friction duration is directly proportional, where the more significant the chamfer angle, the longer it takes for the workpiece to reach its melting point. It is due to the smaller heat input value generated due to the frictional surface area and the maximum surface velocity at the surface. The outer edge of the friction plane gets slower so that less heat is generated, which causes the time needed to connect the workpiece to be longer [1].

Figure 8 shows the results of measuring the flash height and width dimensions after welding using an upright bar-plate rotary friction welding machine. Figure 8 (a) shows a smaller flash height due to adding a chamfer angle. Figure 8 (b) shows a smaller flash height due to a chamfer angle. Figure 8 (a) shows the flash height data. The variation without the chamfer angle produces an average flash height of 2.69 mm. The 15° chamfer angle variation produces an average flash height of 1.64 mm, successfully reducing the flash height by 40% of the variation without the chamfer angle. At 30° chamfer angle variation resulted in an average flash height of 1.43 mm, succeeded in reducing the flash height by 47% from the variation without chamfer angle, and at 45° chamfer angle variation resulted in an average height flash of 1.03 mm managed to reduce the flash height by 62% of the variation without chamfer angle. Figure 8 (b) shows the flash width data. The variation without the chamfer angle produces an average flash width of 1.12 mm. The 15° chamfer angle variation produces an average flash width of 1.04 mm, successfully reducing the flash width by 8% of the variation without the chamfer angle. At 30° chamfer angle variation resulted in an average flash width of 56 mm, succeeded in reducing the flash width by 50% of the variation without chamfer angle, and at 45° chamfer angle variation resulted in an average flash width of 0.26 mm managed to reduce the flash width by 77% of the variation without chamfer angle.

It can be concluded that the variation of the chamfer angle on the different bar surfaces affects the flash height and the width of the resulting flash. The greater the variation of the chamfer angle resulted in a smaller size of the flash produced. It is due to the welding process. The pressure and rotational speed cause the friction surface that has reached the melting point to overflow because it cannot withstand the pressure applied and fills the space due to the creation of different chamfer angles [7],[19-22].

3.2 Non-Destructive Test (NDT) Result

Figure 9 shows a photo of the NDT test results. Figure 9 (a) shows photos of NDT test results without variations in angle, Figure 9 (b) shows photos of NDT test results with 15° chamfer angle variations, Figure 9 (c) shows photos of NDT test results with 30° chamfer angle variations, and Figure 9 (d) shows a photo of the NDT test results with a chamfer angle variation of 45°. At point a show the observation area around the flash, from the results of the NDT test at this point no cracks were found from all variations of the chamfer angle. At point b shows the observation area for the specimen bar area, at this point there are also no cracks found from all variations of chamfer angles. Point c shows the observation area around the specimen plate, and at this point no cracks were found from all variations of the chamfer angle.

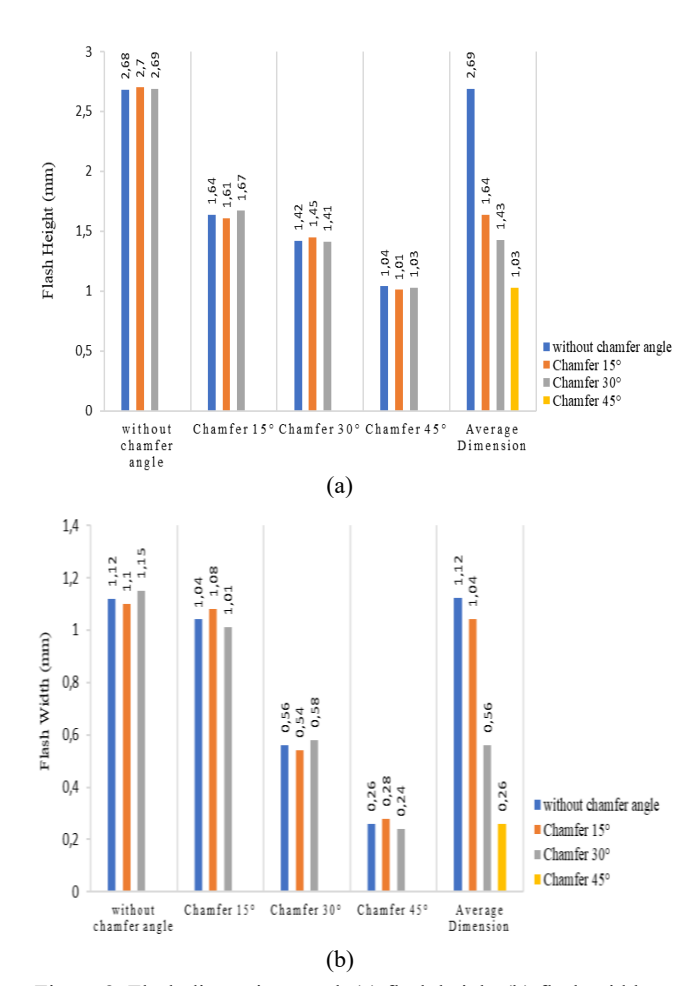


Figure 8: Flash dimension graph (a) flash height (b) flash width

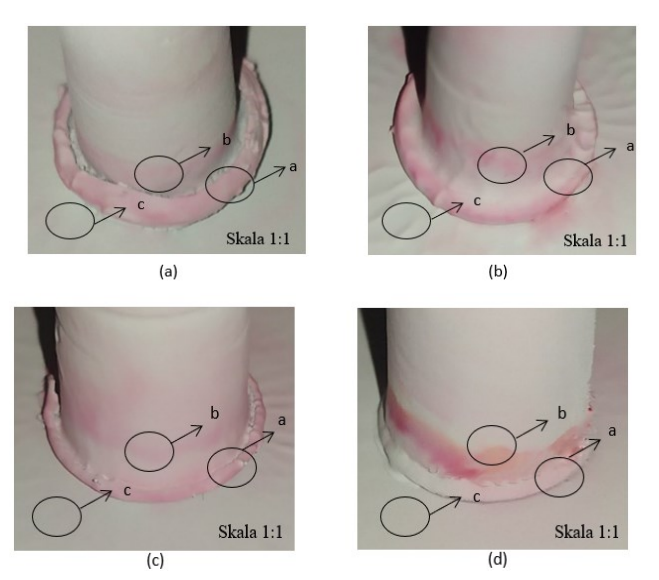


Figure 9: Liquid Penetrant Test (NDT) (a) variation without chamfer angle (0° or 180°), (b) variation of chamfer angle 15°, (c) variation of chamfer angle 30°, and (d) variation of 45° chamfer angle

30th November 2023. Vol.67 No.3 © 2012 ISOMAse, All rights reserved

November 30, 2023

Cracks on the surface are caused by applying a forging pressure that was too high and can also be caused when welding occurs vibrations in the chuck (static material holder), which was rubbed against the material rotating on the spindle. It can be concluded that variations in the chamfer angle using the rotary friction welding bar-plate method have no effect on surface cracking.

3.3 Macro-Observation Result

Figure 10 shows a photo of macro-observations in the interface area. Figure 10 (a) shows macro-observations on specimens of variation without chamfer angles that do not show any void. Figure 10 (b) shows macro-observations on specimens of 15° chamfer angle variations, which do not show any voids. Figure 10 (c) shows macro-observations on the 30° chamfer angle variation specimen, which shows no void. Figure 10 (d) shows macro-observations on specimens with a chamfer angle variation of 45°, which shows no void.

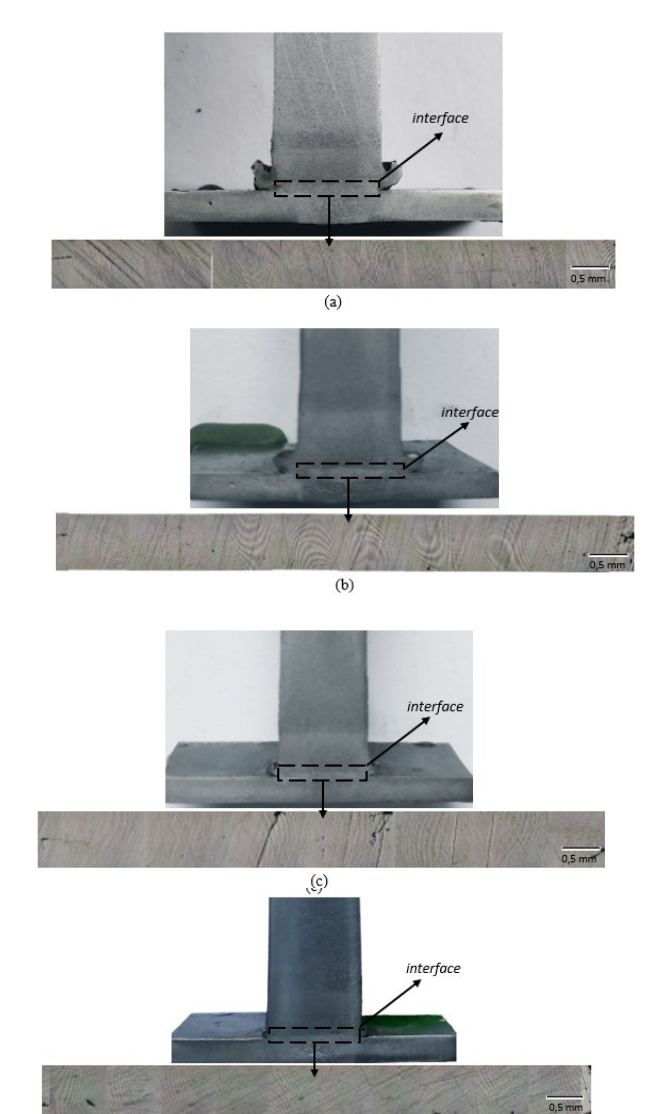


Figure 10: Macro structure (a) variation without chamfer angle (0° or 180°), (b) variation of chamfer angle 15°, (c) variation of chamfer angle 30°, and (d) variation of chamfer angle 45°

In Figure 10, the results of macro-observations did not find any void in the interface area for all variations of the chamfer angle. Therefore, it can be concluded that the cavity in the interface area is shaped like an empty gap that does not merge, and this cavity is not found in the results of macro-observations in the interface area for all variations of chamfer angles. Voids are caused by giving the spindle rotation parameter too low or applying too low a pressure.

3.3 Micro-Observation Result

Figure 11 shows a photo of the difference in microstructure in the base metal, HAZ and weld metal areas that occur in AISI 1037 steel after welding using variations of chamfer angles.

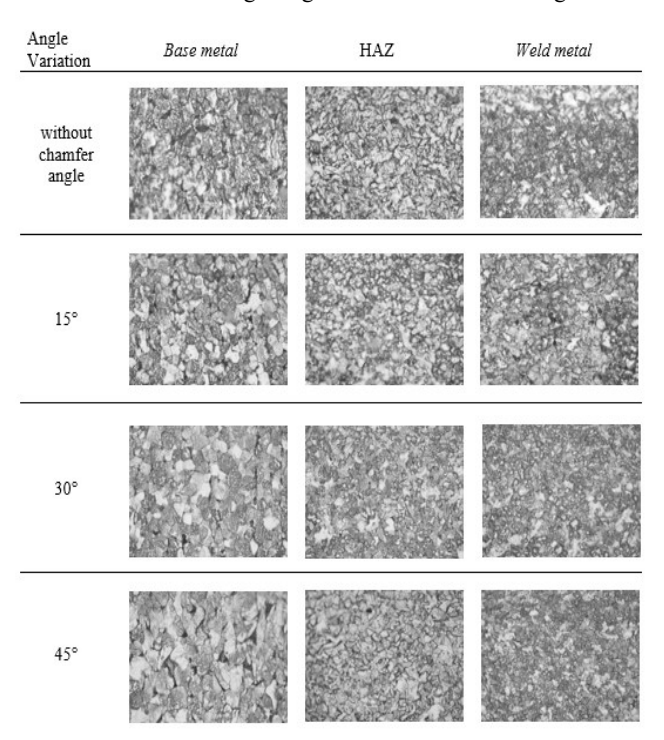


Figure 11: Micro-observation

It can be seen in Figure 11, the observations of the microstructure 50x scale $50\mu m$. There were changes in the microstructure in each region. In the microstructure, the weld metal area experienced grain growth, where the grains were closer together, indirectly causing the grains to be finer than those in the AISI 1037 steel base metal area. It caused the hardness value to increase.

3.4 Hardness Test Result

The result of hardness testing was carried out on five welding areas as shown in Figure 11. It can be seen in Figure 11 the average hardness of the specimen. Overall, the highest hardness test results in the WM (weld metal) area were found in the chamfer angle variation of 45° with an average hardness value of 165.45 VHN. The lowest hardness test results were found in variations without chamfer angles with an average hardness value of 151.58 VHN. As for the HAZ area, the hardness test results showed that the hardness in the HAZ area was higher than the base metal area. The hardness test results indicated that using a larger chamfer angle and longer friction time will produce an optimal hardness value. It can happen

-Science and Engineering-0th November 2023, Vol.67 No.:

30th November 2023. Vol.67 No.3 © 2012 ISOMAse, All rights reserved

because the heat input that occurs during the welding process will affect the metallurgical structure of AISI 1037 mild steel, especially in the weld metal area.

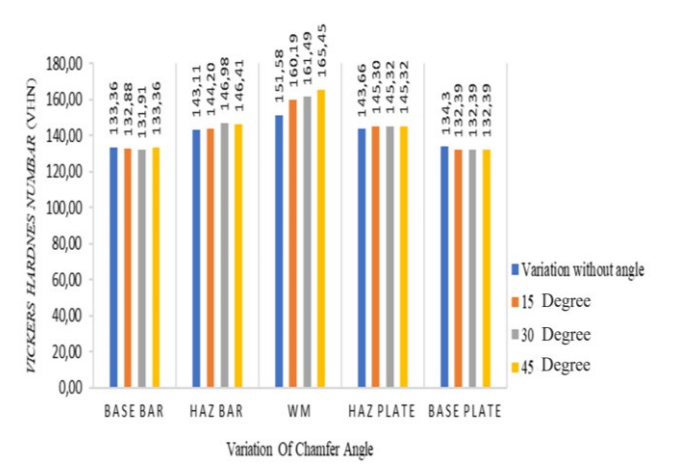


Figure 11: The average hardness test value each variation of chamfer angle

4.0 CONCLUSION

From the study results, the variation of the chamfer angle on different bar surfaces affects the flash height and width of the resulting flash. The greater the variation of the chamfer angle on the given bar surface can be, the smaller the size of the resulting flash. The smallest flash dimension was produced at a chamfer angle variation of 45°. The average flash height was 1.03 mm, reducing flash height by 62% from variations without chamfer angles. An average flash width of 0.26 mm reduces the flash width by 77% of the variation without a chamfer angle. In terms of welding time, it can be concluded that the greater the chamfer angle, the longer the friction time. The fastest average welding time was obtained from variations without chamfer angles, with an average welding time of 40 seconds. The longest average welding time was obtained from variations in the chamfer angle of 45° with an average welding time of 358 seconds. In observing the interface area, the variation of the chamfer angle on different bar surfaces did not affect cracks and voids where all specimens were not found cracks or voids. The chamfer angle variation affects the average hardness value, where the highest hardness was found in the 45° chamfer angle variation in the WM (Weld Metal) area. Meanwhile, the lowest hardness test result was found in variations without chamfer angles in the WM area variations without chamfer angle.

REFERENCES

- [1] Detra, M.R, Yohanes, dan Abdurrahman, R. (2021). Pengaruh sudut chamfer terhadap timing melt point pada penyambungan material mild steel menggunakan las gesek rotary. *JOM FTEKNIK* 8(1).
- [2] Kumar Rajak, D., Pagar, D.D., Menezes, P.L. & Eyvazian, A. (2020). Friction-based welding processes: friction welding and friction stir welding. *Journal of Adhesion Science and Technology*, 34(24), 2613-2637.

- [3] Akinlabi, E.T., Mahamood, R.M., Akinlabi, E.T. & Mahamood, R.M. (2020). Introduction to friction welding, friction stir welding and friction stir processing. Solidstate welding: friction and friction stir welding processes, 1-12.
- [4] Simorangkir, M., Yohanes, Y. & Badri, M. (2023). Effect of spindle speed of bar-plate rotary friction welding machine on joint interface area and hardness value. *Journal of Ocean, Mechanical and Aerospace Science and Engineering-*, 67(1), 34-39.
- [5] Yohanes, Y., Siregar, E., Susilawati, A. & Badri, M. (2018). Performance analysis of flywheel addition on drive system of rotary friction welding machine. *Journal of Ocean, Mechanical and Aerospace -Science and Engineering-*, 52(1), 14-19.
- [6] Yohanes, Y. & Meipen, M. (2022). Effect of rotational speed on hardness value and area of vertical bar-plate rotary friction weld joint. *Journal of Ocean, Mechanical* and Aerospace -Science and Engineering-, 66(3), 77-81.
- [7] Nadya, M, Irawan, Y.S & Choiron, M.A. (2020). Pengaruh double chamfer terhadap flash pada sambungan las gesek al6061 dengan simulasi komputer. Seminar Nasional Teknologi Fakultas Teknik, 2(1), 168-170.
- [8] Murali, K., Ajeetha, A., Ganeshkumar, D., Kumar, R.P. & Viswanathan, M. (2021). Investigation of mechanical properties of dissimilar metals by friction welding. *International Research Journal of Engineering and Technology (IRJET)*, 8(4), 2266-2273.
- [9] Smith, E.H. & Arnell, R.D. (2014). The prediction of frictional temperature increases in dry, sliding contacts between different materials. *Tribology Letters*, 55, 315-328.
- [10] Gandra, J., Krohn, H., Miranda, R.M., Vilaça, P., Quintino, L. & Santos, J.F. (2014). Friction surfacing—A review. *Journal of Materials Processing Technology*, 214(5), 1062-1093.
- [11] Balta, B., Arici, A.A. & Yilmaz, M. (2016). Optimization of process parameters for friction weld steel tube to forging joints. *Materials & Design*, 103, 209-222.
- [12] Shinde, G. & Dabeer, P. (2017). Review of experimental investigations in friction welding technique. Sustainable Development, 373, 384.
- [13] Salih, F I., Dawood, A.S. & Hamid, A.A. (2022). Effects of key processing parameters of continuous drive rotary friction welding on thermal characteristics of similar and dissimilar joints. *Al-Rafidain Engineering Journal* (AREJ), 27(1), 116-126.
- [14] Nu, H.T.M., Loc, N.H. & Minh, L.P. (2021). Influence of the rotary friction welding parameters on the microhardness and joint strength of Ti6Al4V alloys. Proceedings of the Institution of Mechanical Engineers, Part B: Journal of Engineering Manufacture, 235(5), 795-805.
- [15] Utamar, F. & Siswanto (2014). Perancangan dan Pembuatan Mesin Las Gesek Rotary Tegak Bar-plate. Tugas Akhir, Universitas Riau.
- [16] Partomuan, P. & Yohanes (2019). Pengaruh variasi bentuk permukaan *forging* sambungan las gesek *rotary* terhadap kekuatan tarik baja *mild steel. Jom FT EKNIK* 3(2).
- [17] Meng, X., Huang, Y., Cao, J., Shen, J. & dos Santos, J.F. (2021). Recent progress on control strategies for inherent issues in friction stir welding. *Progress in Materials Science*, 115, 100706.



Journal of Ocean, Mechanical and Aerospace

-Science and Engineering-

30th November 2023. Vol.67 No.3 © 2012 ISOMAse, All rights reserved November 30, 2023

- [18] Uzkut, M., Ünlü, B.S., Yilmaz, S.S. & Akdağ, M. (2010). Friction welding and its applications in today's world. In *Proceedings of the 2nd International Symposium on Sustainable Development* (pp. 8-9). Sarajevo: International Burch University.
- [19] Thomas, W.M. (1998). Friction stir welding and related friction process characteristics. In *Proc. 7th Int. Conf. on 'Joints in aluminium–INALCO* (Vol. 98, pp. 157-174).
- [20] Risonarta, V.Y., Ma'arif, M.S. & As'ad, A.F. (2021). Artificial aging heat treatment post-effect on profile and
- mechanical properties of the AA 6061 friction welding joint. In *IOP Conference Series: Materials Science and Engineering*, 1034(1), p. 012134). IOP Publishing.
- [21] Hynes, N.R.J. & Velu, P.S. (2018). Effect of rotational speed on Ti-6Al-4V-AA 6061 friction welded joints. *Journal of manufacturing processes*, 32, 288-297.
- [22] Meschut, G., Merklein, M., Brosius, A., Drummer, D., Fratini, L., Füssel, U., ... & Wolf, M. (2022). Review on mechanical joining by plastic deformation. *Journal of Advanced Joining Processes*, 5, 100113.